

Paraxial design of four-component zoom lens with fixed distance between focal points by matrix optics

ZICHAO FAN¹, SHILI WEI², YAN MO², ZHENGBO ZHU^{2,*}, AND DONGLIN MA^{2,*}

¹MOE Key Laboratory of Fundamental Physical Quantities Measurement & Hubei Key Laboratory of Gravitation and Quantum Physics, PGMF and School of Physics, Huazhong University of Science and Technology, Wuhan 430074, China

²School of Optical and Electronic Information and Wuhan National Laboratory for Optoelectronics, Huazhong University of Science and Technology, Wuhan 430074, China

*zhuzb@hust.edu.cn

*madonglin@hust.edu.cn

Abstract: The initial optical design for the multi-component zoom optical system with fixed distance between focal points is challenging but rewarding. Here, we propose a systematic approach to tackle this problem via matrix optics for the four-component zoom system. The main aim of this paper is to obtain the optimization starting point of four-component zoom system and determine the zoom trajectory. In the design process, the properties of the system matrix of zoom system are analyzed by paraxial ray tracing. Zoom conditions are implemented by restricting the specific matrix elements, and the zoom trajectory is determined by solving the zoom equations iteratively. The efficiency of the proposed method is demonstrated through three numerical examples under two different structures, including a design example with an 8X zoom capability. The results show that the zoom capability has a significant improvement. We believe that the proposed method is a practical and powerful tool for the paraxial design of complex zoom optical systems.

1. Introduction

Zoom optical systems have been widely used in many fields because of the property of variable focal length which enables them to adapt to a variety of working situations [1-3]. In some cases, we are much more concerned about keeping the two foci fixed instead of maintaining a fixed conjugate distance. For instance, a zoom system with fixed focal planes is preferred in the field of optical information processing and machine vision [4-6]. Such zoom lenses are usually used in 4-*f* systems with variable magnification or as a part of double-side telecentric lenses with variable magnification. It has been proved that the number of optical components for such a lens system always exceeds two [7]. For zoom optical systems design, Gaussian brackets and purely algebraic methods [8] are acknowledged as effective methods to perform the theoretical analysis of paraxial properties [9-11]. However, the mathematical derivation becomes extremely complicated for the multi-group zoom optical system, especially when there are more than three groups. Miks *et al.* [12] pioneered the work to simplify the problem based on Gaussian brackets method with a highly symmetric model, but it could not significantly improve the zoom capability for a larger number of components with this configuration. Besides, the paraxial structural design method is also a promising alternative which can directly decide the zoom system's performance, especially for the zoom capability. Once a paraxial structural design is determined via the above mentioned methods, the subsequent optimization with optical software cannot further improve the zoom capability effectively. In other words, the optical performance strongly depends on the initial structure selection. Therefore, it is still a rewarding and urgent task to explore more effective methods to design better initial optical configurations for the zoom optical systems.

Fortunately, the matrix optics method is a powerful tool in dealing with the initial configuration of optical systems, especially for the determination of paraxial structure of

complex optical systems. Kryszczynski *et al.* have been trying to popularize this method in recent years and made significant contributions to the field [13-16]. They proposed a system matrix differential method to deal with the problem of zoom lens design, but the process is relatively complex. In matrix optics, a complex optical system can be described with a unitary quadratic matrix. Compared with other methods, the matrix description of optical systems is simpler and more general, as the elements of the system matrix are directly related to the first-order parameters of the optical system. Based on paraxial ray tracing, optical powers and spaces between components can be written as optical matrix and transfer matrix, and the imaging process can be regarded as the product of these elementary non-commutative matrices.

In this work, we focus on the problem of initial optical design for the four-component zoom optical system with fixed distance between focal points. Specifically, by calculating the system matrix, we firstly perform the paraxial analysis of the problem and derive equations to calculate the required locations of individual elements of the optical system. Then, the starting point of a four-component zoom system is acquired from a simple three-component zoom system by splitting a specific lens among them. After that, we solve the displacement equation through multiple iterations to obtain the initial paraxial structure with the obtained starting point. Finally, once the paraxial structure is determined, the final zoom optical system is completed by the commercial optical design software.

2. Matrix optics method

2.1 Paraxial ray tracing and system matrix

Firstly, only the marginal ray is considered. We assume that the whole optical system is located in the air ($n = n' = 1$). Figure 1 describes the case of paraxial imaging where the marginal ray passes through a single thin lens and transfers the height to the next component. According to the paraxial approximation and Gaussian imaging formula, we can obtain the following relations:

$$u = \frac{y}{-l}, \quad u' = -\frac{y}{l'}, \quad (1)$$

$$\frac{1}{l'} - \frac{1}{l} = \frac{1}{f}. \quad (2)$$

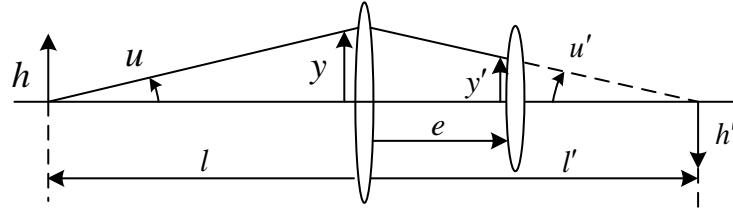


Fig. 1. Paraxial marginal ray coordinates: l, l' - object distance and image distance respectively, e - distance from the current component to the next component, u, u' - paraxial angles identified with the numeric apertures, y, y' - heights of the incident ray on the current and neighbor components

Then we can acquire the paraxial ray tracing formulas and rewrite the equations as a matrix form:

$$\begin{cases} u' = u - y\phi \\ y' = y + eu \end{cases}, \quad (3)$$

$$\begin{cases} R = \begin{bmatrix} 1 & 0 \\ -\phi & 1 \end{bmatrix}, \begin{bmatrix} y \\ u' \end{bmatrix} = R \cdot \begin{bmatrix} y \\ u \end{bmatrix} \\ T = \begin{bmatrix} 1 & e \\ 0 & 1 \end{bmatrix}, \begin{bmatrix} y' \\ u' \end{bmatrix} = T \cdot \begin{bmatrix} y \\ u' \end{bmatrix} \end{cases}, \quad (4)$$

$$\begin{bmatrix} y' \\ u' \end{bmatrix} = T \cdot R \cdot \begin{bmatrix} y \\ u \end{bmatrix}, \quad (5)$$

where R represents the optical power matrix and T denotes the transfer matrix. From Eqs. (3-5), it is clear that the coordinates of the outgoing rays are determined by the incident rays as well as the optical elements. For a thin lens system consisting of n components and two special reference planes, we can get:

$$\begin{bmatrix} y_n \\ u_n \end{bmatrix} = T_n \cdot R_n \cdot T_{n-1} \cdot R_{n-1} \dots T_1 \cdot R_0 \cdot T_0 \cdot \begin{bmatrix} y_0 \\ u_0 \end{bmatrix} = S \cdot \begin{bmatrix} y_0 \\ u_0 \end{bmatrix}, \quad (6)$$

where S is defined as the system matrix, the components and reference planes are labeled as 0, 1, ..., $n+1$ respectively.

2.2 F-F' system and system matrix

In this work, a four-component zoom system with fixed distance between focal points is the primary object to be studied. The reference planes of the system are the front focal plane (FFP) and the back focal plane (BFP), and they do not satisfy the conjugate relation. We call this type of system as F – F' system. For a four-component F – F' system as shown in Fig. 2, there are two particular paraxial rays, including the marginal ray which passes through the front focal point and the parallel ray which enters the system parallelly with respect to the optical axis, being traced separately. From the imaging principles, we can know that the angles $u_0 = \alpha_n = 0$ and the coordinates $H_0 = h_n = 0$. Based on the definition of the system matrix, we obtain the following equation [16]:

$$\begin{bmatrix} 0 & H_n \\ -u_n & 0 \end{bmatrix} = \begin{bmatrix} S_1 & S_2 \\ S_3 & S_4 \end{bmatrix} \cdot \begin{bmatrix} h_0 & 0 \\ 0 & \alpha_0 \end{bmatrix}. \quad (7)$$

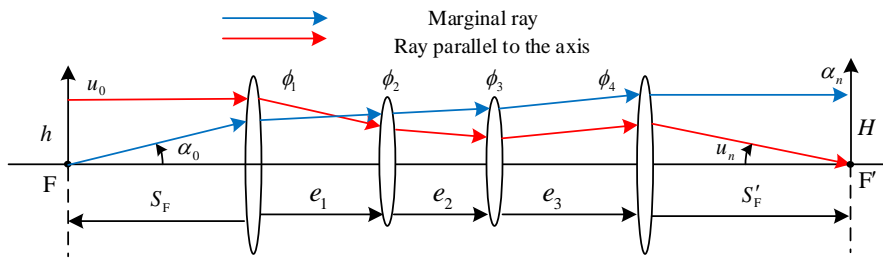


Fig. 2. Characteristics ray coordinates in a four-component F – F' system: F, F' - front focal point and back focal point; $u_0, u_n, \alpha_0, \alpha_n$ - paraxial angles; e - distance from the current component to the next component; S_F - distance from the first thin lens to FFP; S'_F - distance from the last thin lens to the BFP; ϕ - optical power of current component; h, H - height of incident ray.

According to the rules of matrix operation, we can acquire:

$$S_1 \cdot h_0 = 0 \quad ; \quad S_4 \cdot \alpha_0 = 0. \quad (8)$$

$$S_2 \cdot \alpha_0 = H_0 \quad ; \quad S_3 \cdot h_0 = -u_n. \quad (9)$$

From Eq. (8), it is clear that for an F- F' optical system, the selected matrix elements S_1 and S_4 should meet the following requirements:

$$S_1=0 \quad ; \quad S_4=0. \quad (10)$$

Equation (10) ensures that the reference planes are the focal planes of the optical system. Besides, it is not difficult for us to find from Eq. (9) that the geometrical interpretations of system matrix elements S_2 and S_3 are the optical focal length and the opposite of optical power of the entire system respectively. So, S_2 or S_3 makes a connection between the system matrix and the focal length of the optical system. In such a system, we can always assume that S should have the following form:

$$S = \begin{bmatrix} 0 & f \\ -\phi & 0 \end{bmatrix}. \quad (11)$$

2.3 Starting point

A zoom system with mechanical compensation should relocate its components to change the focal length while maintaining the locations of both focal planes. The constraints for our proposed zoom lens with two fixed foci are quite different from the traditional zoom systems. Compared with the classical zoom systems, limiting the focal planes requires an additional degree of freedom due to the absence of the conjugate relationship between them.

The simplest zoom optical system consists of three independently moving elements. In our previous work [17, 18], we derived the axial displacement equation for initial structure determination and presented an automated design method to achieve a paraxial design by means of PSO algorithm. The zoom trajectory of the system can be uniquely determined once the system parameters including the optical power of each component, the optical length and the focal length are determined. Therefore, it is relatively convenient for us to obtain the starting point of four-component zoom optical system based on the initial structure with three components.

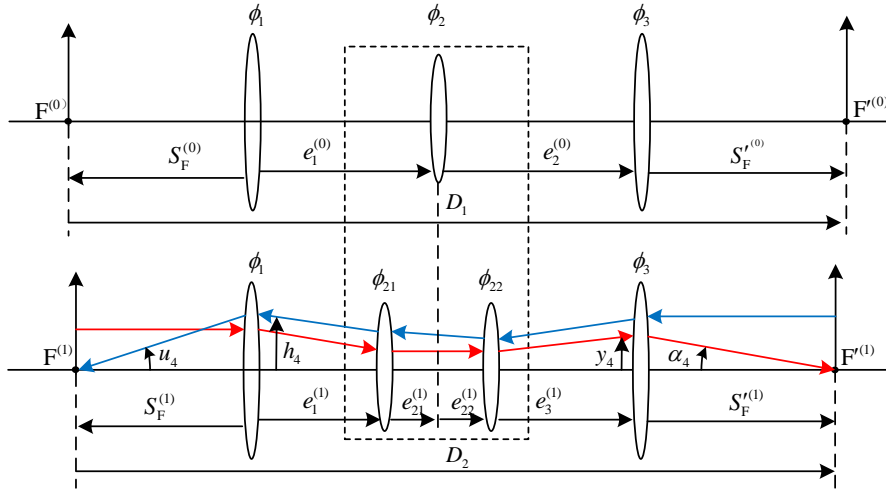


Fig. 3. Split the lens and perform paraxial ray tracing

The process of determining the starting point is illustrated in Fig. 3 [19]. Superscripts 0 and 1 are adopted to distinguish the three-component system from the four-component system. D defines the distance between the two foci, ϕ represents the optical power of individual element, S and e denote the elements' start positions. We split the second component into two independently while maintaining the entire optical power. The individual optical powers, ϕ_{21} and ϕ_{22} , should have the following relationship:

$$\phi_2 = \phi_{21} + \phi_{22} - \phi_{21} \cdot \phi_{22} \cdot (e_{21}^{(1)} + e_{22}^{(1)}). \quad (12)$$

It should be mentioned that in an equivalent Gaussian system containing split components, the object-space principal plane and the image-space principal plane are no longer coincide with each other, thus resulting in a correction of the paraxial parameters. We trace a ray which is parallel to the axis in the forward direction and a ray in the reverse direction, respectively, and acquire S'_F and S_F :

$$S_F^{(1)} = h_4 / u_4 ; \quad S_F'^{(1)} = y_4 / \alpha_4. \quad (13)$$

The other elements' positions can be obtained via geometric relations:

$$e_1^{(1)} = e_1^{(0)} - e_{21}^{(1)} ; \quad e_1^{(1)} = e_2^{(0)} - e_{22}^{(1)}. \quad (14)$$

2.4 Axial displacement equation

For a four-component zoom system with fixed distance between focal points, two stable focal planes and a variable focal length are the stabilization conditions that need to be satisfied simultaneously. It is a fact that only three moving components should be considered to achieve the required stabilization conditions, and it can be realized by presetting a moving trajectory for a specific component. This component is called the active zoom part (AZP). Once the trajectory of AZP is known, the corresponding movement of the other three components can be uniquely determined [13]. The AZP should be selected on the premise that there are no collisions between each component.

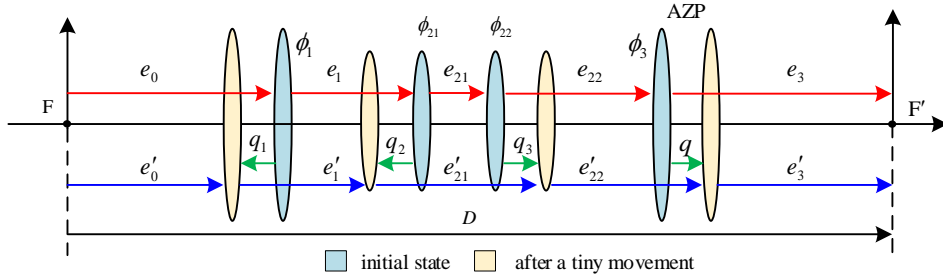


Fig. 4. The movement of the components

The zooming progress of the optical system is schematically illustrated in Fig. 4. The system matrix S_0 of the starting point can be obtained from Eq. (6):

$$S_0 = \begin{bmatrix} 1 & e_3 \\ 0 & 1 \end{bmatrix} \cdot \begin{bmatrix} 1 & 0 \\ -\phi_4 & 1 \end{bmatrix} \cdot \begin{bmatrix} 1 & e_{22} \\ 0 & 1 \end{bmatrix} \cdot \begin{bmatrix} 1 & 0 \\ -\phi_{22} & 1 \end{bmatrix} \cdot \begin{bmatrix} 1 & e_{21} \\ 0 & 1 \end{bmatrix} \cdot \begin{bmatrix} 1 & 0 \\ -\phi_{21} & 1 \end{bmatrix} \cdot \begin{bmatrix} 1 & e_1 \\ 0 & 1 \end{bmatrix} \cdot \begin{bmatrix} 1 & 0 \\ -\phi_1 & 1 \end{bmatrix} \cdot \begin{bmatrix} 1 & e_0 \\ 0 & 1 \end{bmatrix}, \quad (15)$$

where e_0 is the distance from the front focal plane to the first surface, e_3 is the distance from the last surface to the back focal plane. Obviously, $e_0 = -S_F$ and $e_3 = S'_F$. Then a tiny displacement q is added to the active zoom part, thus the other components need to compensate for the offset of the focal planes caused by this displacement. These compensations are represented as the displacements q_1 , q_2 and q_3 . The optical power of each component is invariable in this process, only the elements in the transmission matrix change slightly:

$$T_{14} = \begin{bmatrix} 1 & e_3 - q \\ 0 & 1 \end{bmatrix} ; \quad T_{13} = \begin{bmatrix} 1 & e_{22} - q_3 + q \\ 0 & 1 \end{bmatrix} ; \quad T_{12} = \begin{bmatrix} 1 & e_{21} - q_2 + q_3 \\ 0 & 1 \end{bmatrix} ; \quad (16)$$

$$T_{11} = \begin{bmatrix} 1 & e_1 - q_1 + q_2 \\ 0 & 1 \end{bmatrix} ; \quad T_{10} = \begin{bmatrix} 1 & e_0 + q_1 \\ 0 & 1 \end{bmatrix},$$

where T_{in} is the n -th ($n=0,1\dots4$) transfer matrix after the i -th iteration. Substituting Eq. (16) into Eq. (6), a new system matrix can be obtained:

$$S_i = \begin{bmatrix} 1 & e_3 - q \\ 0 & 1 \end{bmatrix} \cdot \begin{bmatrix} 1 & 0 \\ -\phi_4 & 1 \end{bmatrix} \cdot \begin{bmatrix} 1 & e_{22} - q_3 + q \\ 0 & 1 \end{bmatrix} \cdot \begin{bmatrix} 1 & 0 \\ -\phi_{22} & 1 \end{bmatrix} \cdot \begin{bmatrix} 1 & e_{21} - q_2 + q_3 \\ 0 & 1 \end{bmatrix} \\ \cdot \begin{bmatrix} 1 & 0 \\ -\phi_{21} & 1 \end{bmatrix} \cdot \begin{bmatrix} 1 & e_1 - q_1 + q_2 \\ 0 & 1 \end{bmatrix} \cdot \begin{bmatrix} 1 & 0 \\ -\phi_1 & 1 \end{bmatrix} \cdot \begin{bmatrix} 1 & e_0 + q_1 \\ 0 & 1 \end{bmatrix}. \quad (17)$$

The stabilization condition in a matrix form is implicit in Eq. (11), and the axial displacement equation can be written as:

$$\begin{cases} 0 = S_{i+1}[1,1] - S_i[1,1] \\ 0 = S_{i+1}[2,2] - S_i[2,2] \\ \Delta f = S_{i+1}[1,2] - S_i[1,2] \end{cases}. \quad (18)$$

The values of q_1 , q_2 and q_3 can be obtained numerically by solving Eq. (18). For each iteration, the effective focal length of the whole system increases Δf . The zoom speed depends on the Δf and q . For the value selection of these two parameters, a faster zoom speed is preferred under the premise of ensuring the zoom trajectory smooth.

In summary, the whole design process for a prescribed zoom system is shown in Fig. 5. In the middle of the process of the whole design process, if the optimized system does not meet the predefined requirements, designers need to split the lens again or choose another initial design of three components system. The recommended zoom trajectory should be as smooth as possible. Besides, a compact optical space is also preferred.

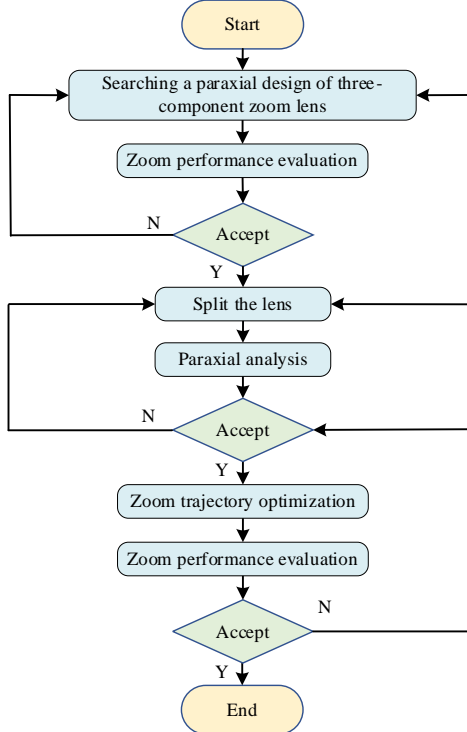


Fig. 5. Flow chart of design process

3. Numerical examples

3.1 FFP lays outside of the system

In the first design example, we select a three-component zoom system whose FFP lays outside of the system as the seed and the design parameters are listed in Table 1. As a fact that it is very difficult to find the initial structure without rich experience. In this work, a relatively well-behaved structure retrieving method based on the PSO algorithm, which is detailed in our previous work [17], is adopted for the subsequent design work.

Table 1. The design data of 2X three-component zoom system (Unit: mm)

$f_1 = 51.4026; f_2 = -16.3082; f_3 = 23.8663; D = 81.8341$				
f	e_0	e_1	e_2	e_3
32.44	7.69	0.57	17.82	55.57
38.93	3.03	8.74	17.03	53.03
45.42	0.81	14.39	16.05	50.58
51.90	0.21	19.07	15.08	47.47
58.39	1.03	23.32	14.15	43.33
64.88	3.34	27.49	13.21	37.78

We slip the second component into two thin lenses with negative optical power, then the whole system has the structure of PNNP (P represents a positive optical power of the component, and N stands for a negative optical power of the component). For such a symmetry structure with the ability to compensate field curvature, it is generally easy to control the aberration in the subsequent optimization [9-10, 20]. According to Eqs. (12) - (14), the values of each optical power matrix and transfer matrix can be obtained. The design data of the starting point is listed in Table 2. f_0 is the focal length of the starting point, and the 4th component is chosen as the AZP in this design.

Table 2. The design data of starting point

$f_0 = 36\text{mm}; D = 86.804\text{mm}; \text{AZP: the 4}^{\text{th}} \text{ component}$					
Distance (mm)	e_0	e_1	e_2	e_3	e_4
	9.73	0.57	3	14.82	58.68
Optical power (mm ⁻¹)	ϕ_1	ϕ_2	ϕ_3	ϕ_4	
	0.0195	-0.0333	-0.0262	0.0419	

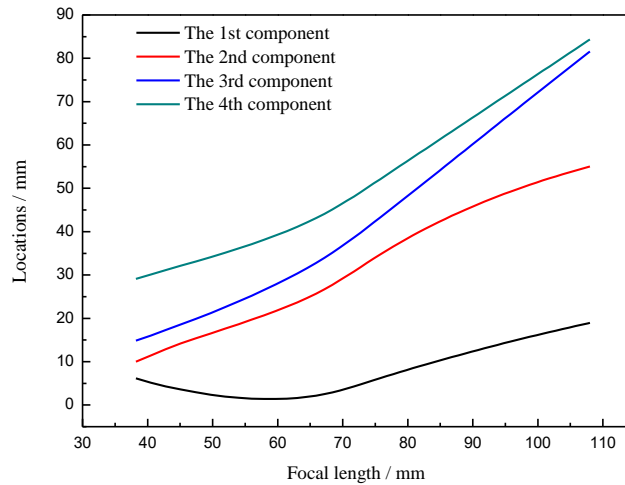


Fig. 6. Loci of the four components

Table 3. The design data of 3X four-component zoom system (Unit: mm)

$f_1 = 51.4026; f_2 = -30; f_3 = -38.115; f_4 = 23.8663$					
f	e_0	e_1	e_2	e_3	e_4
36.00	9.73	0.57	3.00	14.82	58.68
47.40	2.37	14.16	4.71	12.89	52.68
59.70	1.40	20.29	6.12	11.31	47.68
72.76	4.75	27.09	7.96	9.32	37.68
84.77	10.21	32.02	11.72	7.18	25.68
96.77	14.99	34.78	18.51	4.83	13.68
108.00	18.95	36.07	26.55	2.78	2.45

Equation (18) needs to be solved several times during the design process, where the absolute value of q is set to be 0.1mm in each iteration. By adjusting the changing rate of the focal length and the movement direction of AZP to ensure a smooth zoom trajectory. Besides, no collisions between each component should also be guaranteed. Implementing the iterations until meeting the predefined design requirements. The final zoom trajectory is illustrated in Fig. 6. This figure shows that a smooth zoom trajectory has been achieved.

Figure 7 describes the layout of the zoom system with a small field of view including a short, a medium and a long focal length cases. In Fig. 8, we use actual lenses to replace the ideal paraxial surfaces to verify the effectiveness of the obtained paraxial design. The result shows that the paraxial design can provide a reliable starting point for subsequent optimization.

Without loss of generality, we split the third lens of the same seed and make subsequent optimizations. The starting point information is listed in Table 4. We set $e_3 = 5$ to make an adequate spatial room for the movement of the components. The optical power of the component in the system is allocated as PNPP. The results of the design are listed in Table 5 and the zoom trajectory is depicted in Fig. 9, where the zoom trajectory is completely different from the previous one. Besides, different selections of starting point as well as AZP may also lead to different optimization results.

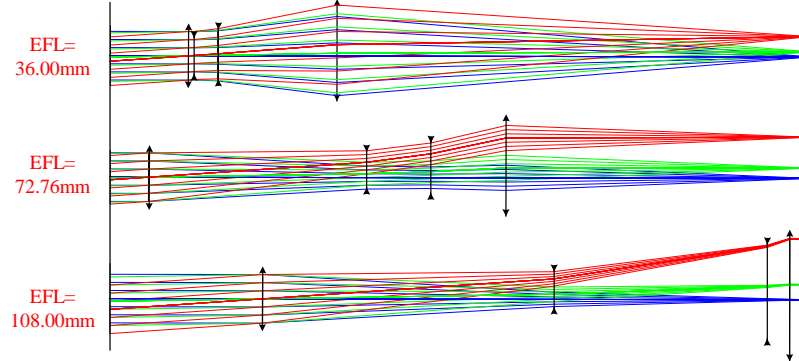


Fig. 7. Diagram of the 3X four-component zoom $F-F'$ system at the sampled position

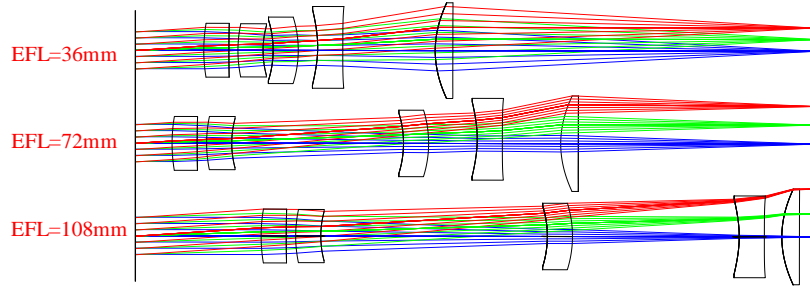


Fig. 8. Layout of the zoom system with an actual lens at the sampled position

Table 4. The design data of starting point

$f_0 = 33.55\text{mm}; D = 83.26\text{mm}; \text{AZP: the 4}^{\text{th}} \text{ component}$					
Distance (mm)	e_0	e_1	e_2	e_3	e_4
	9.01	0.57	14.82	5	53.86
Optical power (mm ⁻¹)	ϕ_1	ϕ_2	ϕ_3	ϕ_4	
	0.0195	-0.0613	0.025	0.0193	

Table 5. The design data of 3X four-component zoom system (Unit: mm)

$f_1 = 51.4026; f_2 = -16.3082; f_3 = -40; f_4 = 51.7749$					
f	e_0	e_1	e_2	e_3	e_4
33.55	9.01	0.57	14.82	5	53.86
47.32	4.28	15.14	13.05	2.93	47.86
59.58	6.95	24.83	11.44	1.17	38.86
72.52	8.58	32.02	9.51	6.29	26.86
84.93	10.33	35.56	7.12	14.39	15.86
99.62	15.14	37.68	3.63	23.95	2.86

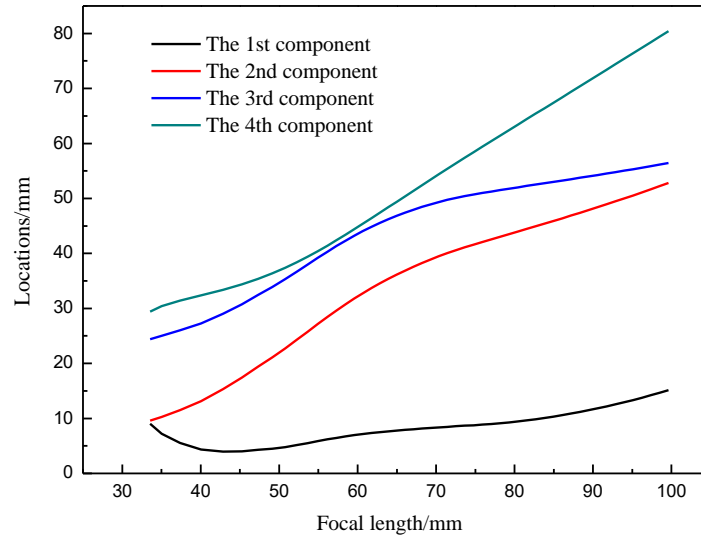


Fig. 9. Loci of the four components

3.2 FFP lays inside of the system

In the second example, another possible structure with an FFP located inside the system is considered. Of course, an additional prime lens can be employed to transfer the FFP out of the system if needed, at the expense of increasing the optical length of the system. For this design example, the only difference from the first design example is that e_0 is negative considering the law of symbols. As shown in Fig. 10, due to the calculation of the system matrix is not affected by the inner front focal plane, the sequence of ray tracing can be considered to start from the reference plane. When we calculate the system matrix, the light ray can be thought of being traced from the front focus, so the system matrix of this structure is the same as the previous one.

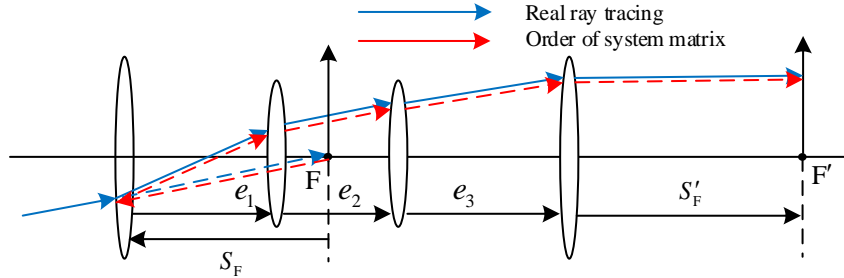


Fig. 10. The tracing sequence in an optical system that FFP lays inside of the system

Table 6. The design data of 4X three-component zoom system (Unit: mm)

$f_1 = 70.9968; f_2 = -15.3704; f_3 = -22.7324; D = 75.2318$				
f	e_0	e_1	e_2	e_3
29.57	-4.73	7.81	19.97	52.19
51.75	-21.44	27.97	16.15	52.55
73.93	-25.27	40.13	13.77	46.60
96.10	-19.85	50.92	23.01	32.14
118.28	-0.38	64.56	10.33	0.73

Similarly, the design of the zoom system starts with generating a favorable starting point. The design parameters of a 4X three-component F- F' zoom system are listed in Table 6. The second component of the three-component system is divided into two independent moving components. With the procedure of trial and error, two components with optical power ϕ_2 and ϕ_3 are placed on both sides of the FFP respectively, which perhaps has more possibility to get a higher zoom ratio. The first component, the second component, FFP, the third component and the fourth component are arranged in order along the optical axis. We choose the fourth component as AZP. The data of the starting point is listed in Table 7.

Table 7. The design data of starting point

$f_0 = 26.0180\text{mm}; D = 73.1077\text{mm}; \text{AZP: the 4}^{\text{th}} \text{ component}$					
Distance (mm)	e_0	e_1	e_2	e_3	e_4
	-4.57	1.78	7	18.97	49.93
Optical power (mm ⁻¹)	ϕ_1	ϕ_2	ϕ_3	ϕ_4	
	0.0141	-0.025	-0.0341	0.0440	

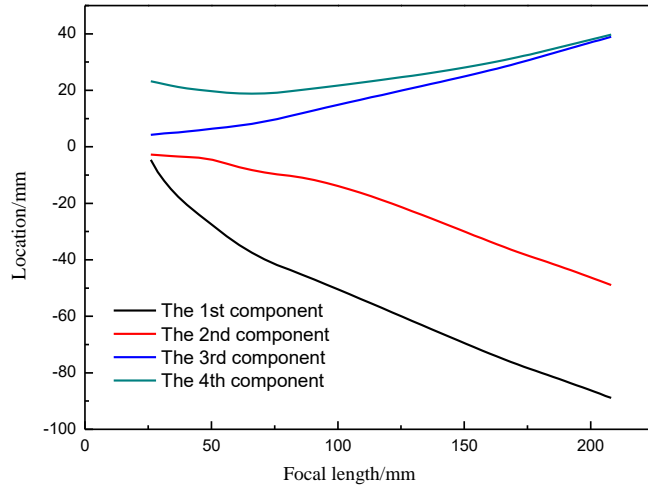


Fig. 11. Loci of the four components

Table 8. The design data of 8X four-component zoom system (Unit: mm)

	$f_1 = 70.9968$	$f_2 = -40$	$f_3 = -29.3309$	$f_4 = 22.7324$	
f	e_0	e_1	e_2	e_3	f
26.02	-4.57	1.78	7	18.97	49.93
50.52	-27.81	23.20	11.03	13.25	53.43
85.92	-45.29	34.38	22.84	8.25	52.93
121.52	-58.59	38.45	39.31	5.01	48.93
157.02	-72.08	39.62	58.85	2.78	43.93
182.82	-80.71	39.94	73.34	1.62	38.93
208.12	-88.87	39.97	87.86	0.71	33.43

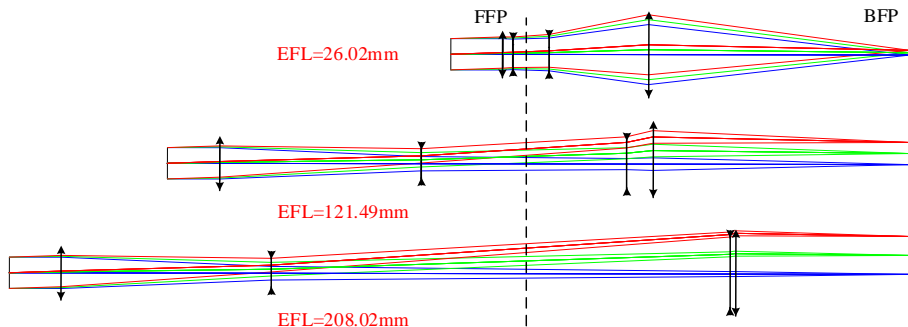


Fig. 12. Diagram of the 8X four-component zoom F- F' system at the sampled position

In the zooming process, AZP firstly moves in the opposite direction of the optical axis and then forward. The zoom trajectory is shown in Fig. 11. The first two components and the second two components never pass through the FFP, where a real aperture stop or spatial filters can be placed if needed. Table 8 lists the data of a specific sampling position on the zoom curve. Figure 12 describes the layout of the zoom system with a small field of view including a short, a medium and a long focal length case. The distance between FFP and BFP is constant, and the maximum optical length is 161.98mm.

4. Conclusion

In this paper, a systematic approach using matrix optics for the paraxial design of an F- F' zoom lens system is presented. Compared with the traditional analysis method, the matrix optics method is more concise to deal with the problem of multi-component zoom system, because the entire optical system can be regarded as a black box when the axial displacement equation is constructed. With the help of the PSO algorithm which has been proved efficient in our previous work, we obtain the three-component system quickly. Then, the starting point of the four-component system is acquired by splitting a specific lens of the three-component system. After that, the kinematics inside the black box is analyzed by adjusting one of the components, we call AZP, to optimize the zoom trajectory. Three numerical examples show that the proposed method is effective and can be applied to different structures. This highly formalized approach can not only provide a clarity of thought for optical designers, but also build a bridge between the basic three-component configuration with the complex multi-component configuration. In addition, the proposed method can also be extended to the ordinary zoom lens systems or other types of special zoom systems.

Funding

National Natural Science Foundation of China (61805088); Science, Technology, and Innovation Commission of Shenzhen Municipality (JCYJ20190809100811375); Key Research and Development Program of Hubei Province (2020BAB121); Fundamental Research Funds for the Central Universities (2019kfyXKJC040); Innovation Fund of WNLO.

Disclosures

The authors declare no conflicts of interest.

References

1. G. I. Greisukh, E. G. Ezhov, Z. A. Sidiyakina, and S. A. Stepanov, "Design of plastic diffractive–refractive compact zoom lenses for visible–near-IR spectrum," *Appl. Opt.* **52**(23):5843–5850 (2013).
2. Y. Qin, and H. Hua, "Continuously zoom imaging probe for the multi-resolution foveated laparoscope," *Biomed. Opt. Express* **7**(4):1175–1182 (2016).
3. L. Li, D. Wang, C. Liu, and Q. Wang, "Ultrathin zoom telescopic objective," *Opt. Express* **24**(16):18674 (2016)
4. S. Bloch and E. I. Betensky, "Telecentric zoom lens used in metrology applications," *Proc. SPIE* **4487**, 42–52 (2001).
5. G. Baldwin-Olguin, "Telecentric lens for precision machine vision," *Proc. SPIE* **2730**, 440–443 (1996).
6. J. W. Goodman, *Introduction to Fourier Optics* (McGraw-Hill, 1968).
7. A. Miks, J. Novak, and P. Novak, "Three-element zoom lens with fixed distance between focal points," *Opt. Lett.* **37**(12), 2187–2189 (2012).
8. M. Herzberger, "Gaussian optics and Gaussian brackets," *J. Opt. Soc. Am.* **33**:651–652 (1943).
9. K. Tanaka, "Paraxial analysis of mechanically compensated zoom lenses. 1: Four-component type," *Appl. Opt.* **21**(12), 2174–2183 (1982).
10. K. Tanaka, "Paraxial analysis of mechanically compensated zoom lenses 3: Five-component type," *Appl. Opt.* **22**(4):541–553 (1983).
11. K. Yamaji, "Design of zoom lenses", in *Progress in Optics*, **6**: 105–170 (1967).
12. A. Miks, and J. Novak, "Paraxial analysis of four-component zoom lens with fixed distance between focal points," *Appl. Opt.* **51**(21), 5231–5235 (2012).
13. T. Kryszczyński, and J. Mikucki, "Structural optical design of the complex multi-group zoom systems by means of matrix optics," *Opt. Express* **21**(17):19634–19647 (2013).
14. T. Kryszczyński, M. Leśniewski, and J. Mikucki, "New approach to the method of the initial optical design based on the matrix optics", *Proc. SPIE* **7141**:71411X (2008).
15. T. Kryszczyński, and J. Mikucki, "Interactive matrix method for analysis and construction of optical systems with elaborated components," *Proc. SPIE* **7746**, 77461M (2010).
16. T. Kryszczyński, "Development of the double-sided telecentric three-component zoom systems by means of matrix optics," *Proc. SPIE* **7141**, 71411Y (2008).
17. Z. Fan, S. Wei, Z. Zhu, Y. Mo, Y. Yan, and D. Ma, "Automatically retrieving an initial design of a double-sided telecentric zoom lens based on a particle swarm optimization," *Appl. Opt.* **58**(27), 7379–7386 (2019).
18. Z. Fan, S. Wei, Z. Zhu, Y. Mo, Y. Yan, L. Yan, and D. Ma, "Globally optimal first-order design of zoom systems with fixed foci as well as high zoom ratio," *Opt. Express* **27**(26):38180–38190 (2019)
19. J. M. Geary, *Introduction to Lens Design: with Practical ZEMAX*, (Willmann-Bell, 2002).

20. J. Zhang, X. Chen, J. Xi, and Z. Wu, "Paraxial analysis of double-sided telecentric zoom lenses with three components," *Appl. Opt.* **53**(22), 4957–4967 (2014).